ELSEVIER

0308-0161(95)00085-2

Int. J. Pres. Ves. & Piping 66 (1996) 59–76

0308-0161/96/$15.00

EVALUATION OF PREMATURE FAILURE OF A GAS TURBINE COMPONENT

M.O. DEDEKIND and L.E. HARRIS

Division of Materials Science and Technology
CSIR, P.O.Box 395, PRETORIA, 0001, RSA

ABSTRACT

A case study of certain gas turbine stator vanes which fail prematurely is presented, with a view to determining whether operational procedure might have caused the failures. The engines had been operated from a 'hot-and-high' environment, and this could have contributed to the failures.

Computational fluid dynamics (CFD) techniques were employed in order to obtain an accurate design point thermal history. The resulting convection boundary conditions were then interpolated over a finite element mesh. Transient thermal and stress analyses were performed. At the same time, microstructural analyses of the service-exposed material were carried out to estimate the maximum temperature seen by the component. These showed that higher than expected vane metal temperatures were experienced. Emphasis was placed on the procedures outlined in the USAF Engine Structural Integrity Program[1], since little detail was known about the actual engine operating histories.

KEYWORDS

Life assessment; MAR-M509; Gas turbine engines; CFD; finite element analysis.

NOMENCLATURE

a	crack length
E	Young's modulus
k	heat transfer coefficient
N	number of cycles
N_f	cycles to failure
t	time
T	temperature
α	coefficient of thermal expansion
ε	strain
ε_f	strain to failure
σ_{UTS}	Ultimate tensile strength

INTRODUCTION

Accurate design life and remaining life prediction has been identified as an important aspect of any gas turbine programme concentrating on such aspects as maintenance, upgrade and repair qualification. Historically, emphasis has been placed on design life prediction, where design life was deemed to have been reached at the initiation of a small crack. However, with the current emphasis on damage tolerant design and maintenance philosophies, there is a need to understand degradation modes, crack initiation as well as propagation lives, and acceptable defect sizes.

Thermo-mechanical fatigue (TMF) has been recognised as a major cause of degradation and failure of gas turbine hot-end components. While significant progress has been made in recent years in predicting the TMF behaviour of materials, there is as yet no generally accepted method of doing so. In addition, an intimate knowledge of material (creep, low cycle fatigue, oxidation and TMF) behaviour is required. However, complete characterization of a material is costly, time-consuming and therefore impractical where quick solutions to everyday operational problems are required.

Because gas turbine operators place emphasis on practical and useable solutions to service problems, a quick but effective analysis process is required. A recent case study in which the nozzle guide vanes of a locally operated military aircraft were subject to premature failure is described. It was important to establish the mode of failure, and to understand the cause of this. Recommendations could then be made on how to prevent further failures in service. Due to budget constraints, however, a full-scale research project could not be attempted. Published materials data had to be used, and assumptions made regarding the operating cycles of the engine.

FAILURE INVESTIGATION

Examples of the retired components were subjected to microstructural investigation to determine the cause of failure. ***Figure 1*** shows a typical retired component, made up of six vanes in a cast stator ring sector. The damaged regions are highlighted in ***Fig. 1***, and consist of fatigue cracks of up to 10 mm in length at the leading and trailing edges. No cracks were visible anywhere else on the component. The material in question is MAR-M509, a cast cobalt-based superalloy commonly used in nozzle guide vanes. In this alloy, the effect of oxidation in localized fatigue damage is particularly significant. MC carbides, which serve to stengthen the alloy, oxidize at service temperatures, and serve as nucleation and preferred propagation paths for fatigue cracks. This damage can become the determining factor in the endurance life even in the absence of visible surface degradation[3].

The microstructural examination showed that the vanes had cracked on the leading and trailing edges, and that this was indeed due to the precipitation of carbides on the grain boundaries and that these had acted as crack initiation sites and crack paths. Although this failure mechanism is operative from around 700°C, the low number of service hours experienced by these components led to the conclusion that the metal temperatures could have been higher than expected.

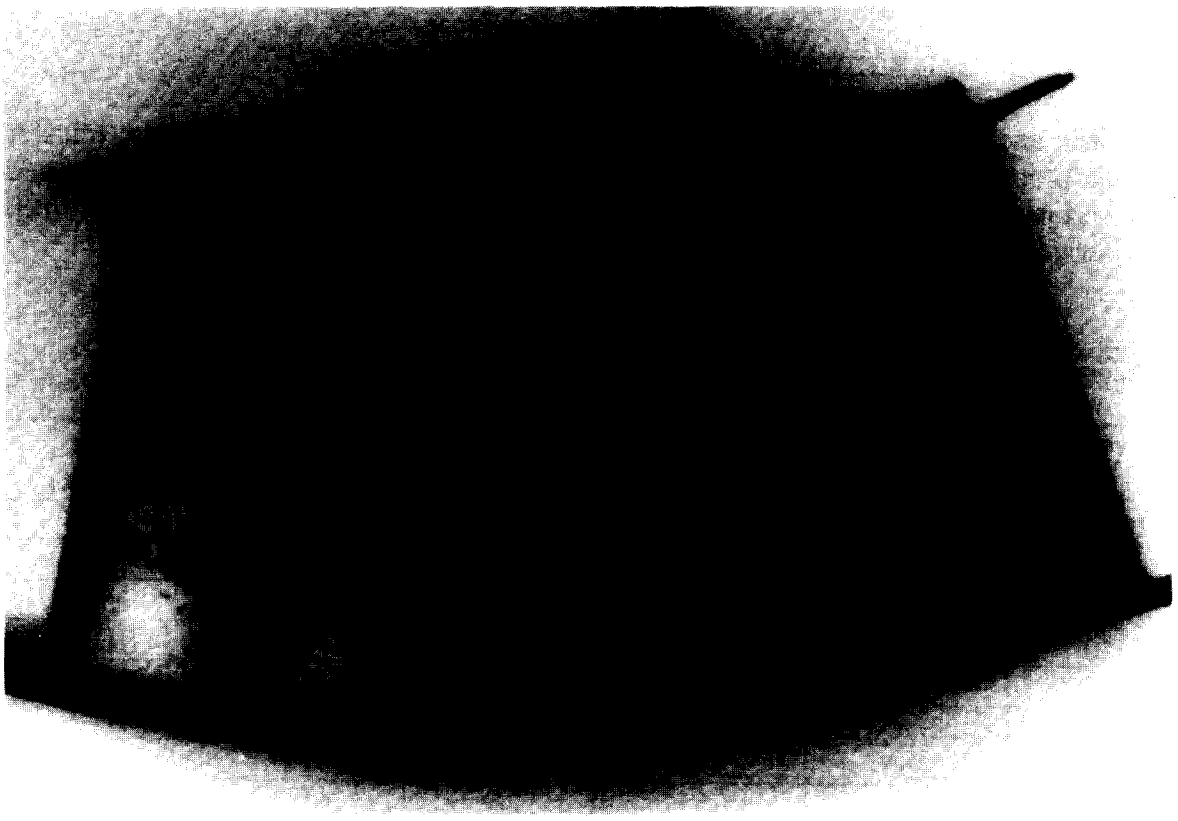

Fig. 1. Photograph of damaged vane sector.

Although it was obvious therefore that failure was due to embrittlement of the material where it was exposed to prolonged high temperatures, which led to the rapid growth of fatigue cracks, it was nevertheless important to the operator of these engines to understand the causes and effects of higher than expected service temperatures, in order to evaluate the damage which might be occurring in other engines operating under similar conditions. It was quite possible that the 'hot-and-high' idle and take-off conditions under which these engines operated had a large effect on the reduced life of the components. For this reason it was decided to model the component using these severe operating conditions.

MATERIAL DATA: MAR-M 509

In order to perform meaningful life prediction analysis, a thorough understanding of the material's behaviour, as well as the failure modes encountered under operating conditions, is necessary. In general this requires an extensive materials testing programme in order to thoroughly characterise the alloy, and this is both time consuming and expensive. Since the stated objective of this investigation was to produce quick and cost effective solutions to problems encountered by engine operators, an intensive literature search was conducted in order to minimise materials testing. Fortuitously, MAR-M509 has been extensively

researched, and it was possible to obtain from the literature data which was far in excess of any that could have been generated locally. The results of this study are presented in this section.

Mechanical, thermal and creep data

In the older and more commonly used alloys like MAR-M509, mechanical, heat transfer and creep property data are easily obtained. ***Tables 1 and 2*** provide the mechanical and thermal property data used in the analysis and ***Fig. 2*** shows the Larson-Miller creep curves derived from the literature.[3-5]

Table 1. Mechanical and Thermal Property Data of MAR-M509.[3]

T (°C)	E (GPa)	σ_{UTS} (MPa)	ε_f (%)	k (W/m/K)	α (μ m/m/K)
21	225	785	4	-	-
205	215	-	-	-	-
425	195	-	-	25.2	15.3
540	-	570	6	27.9	15.9
650	180	560	7	31.1	16.2
760	165	570	10	34.3	16.7
870	155	350	20	37.6	17.2
980	135	560	26	41.2	17.6

Table 2. Mechanical Property Data of MAR-M509.[3]

Density (kg/m³)	Specific Heat (J/kg/K)
8850	440

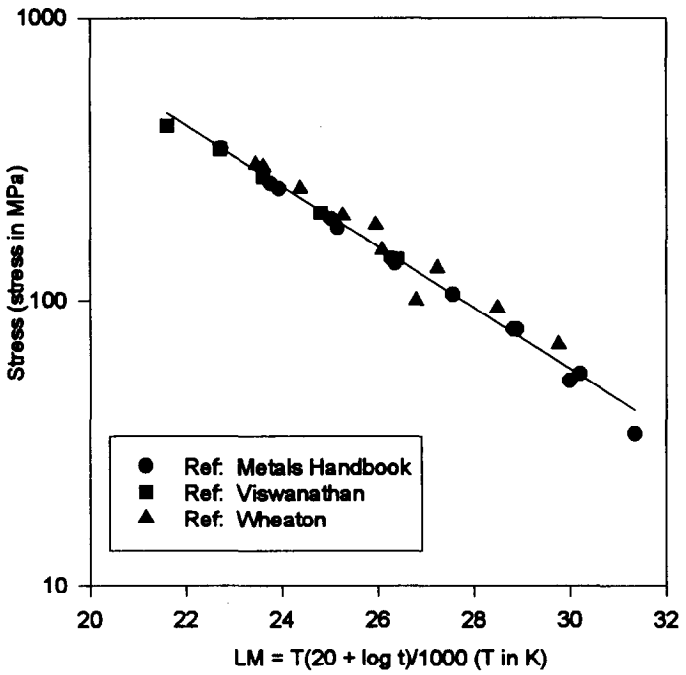

Fig. 2: Larson-Miller Curves of MAR-M509.

Cyclic Behaviour

The behaviour of MAR-M509 under high temperature fatigue, low cycle fatigue, thermal fatigue and thermo-mechanical fatigue is described in references 6-11. In addition, various lifeing algorithms were assessed, and some of these will be described in the next section.

Low cycle fatigue tests in air at 900°C at various frequencies and wave forms have shown that for continuous cycling at the frequencies typically observed in gas turbine components, fatigue life is nearly independent of frequency. Tensile and compressive holds are equally damaging, resulting in a reduction in fatigue life of around 50%. ***Figure 3*** shows the results of this investigation. At low strain ranges, initiation accounted for around half of the total life, where initiation was defined as a crack of depth 0.3mm[7].

In another study[8] isothermal LCF and thermal fatigue lives were compared. This study showed that in both instances failure was due to the mechanism described in the Failure Investigation section, which suggests that a fatigue rather than a creep approach to lifeing is better for the kind of loading experienced by nozzle guide vanes. In this instance, life was determined to be number of cycles to initiation of a 1mm crack. Thermal fatigue was shown to produce considerably shorter fatigue lives than LCF. This is illustrated in ***Fig. 4***.

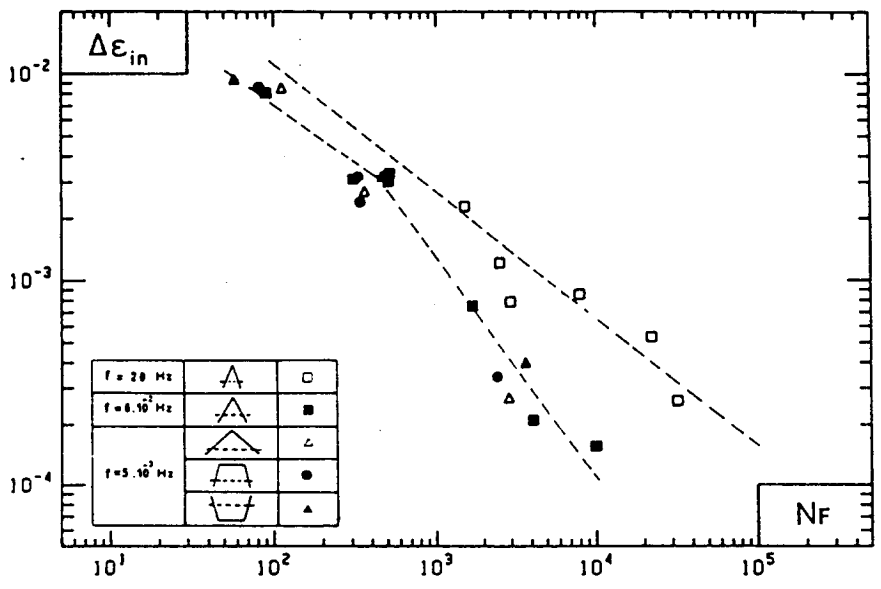

Fig. 3. Number of cycles to failure in low cycle fatigue as a function of the inelastic strain range[7].

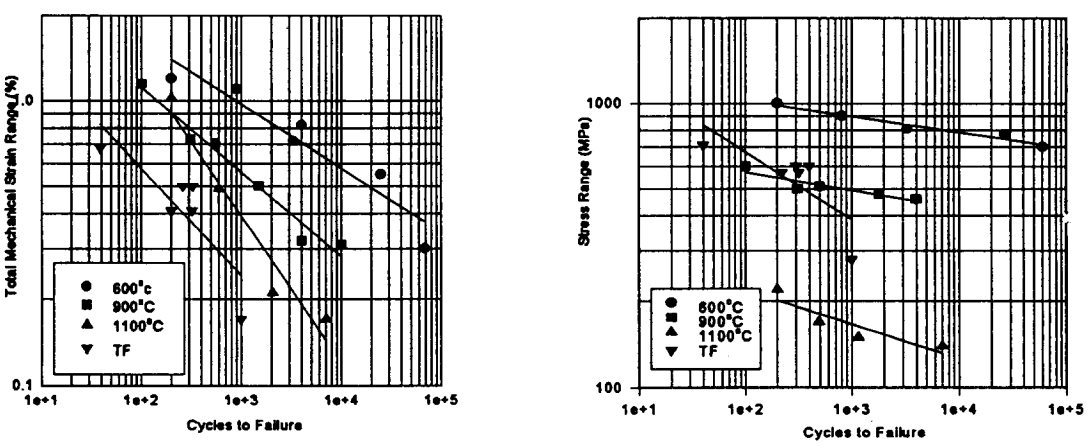

Fig 4. Comparison between thermal fatigue life to 1mm crack depth and low cycle fatigue life at various temperatures as a function of a) total mechanical strain range and b) peak stress range[8].

The LCF life at 900°C was also compared against the TMF life. TMF testing was done in an anti-clockwise diamond waveform, with zero mechanical strains being imposed at 600 and 1050°C and maximum compressive and tensile strains at 900 and 700°C respectively. The results showed that TMF is considerably more damaging than LCF. This is particularly the case at lower strain ranges, and is illustrated in ***Fig. 5***.

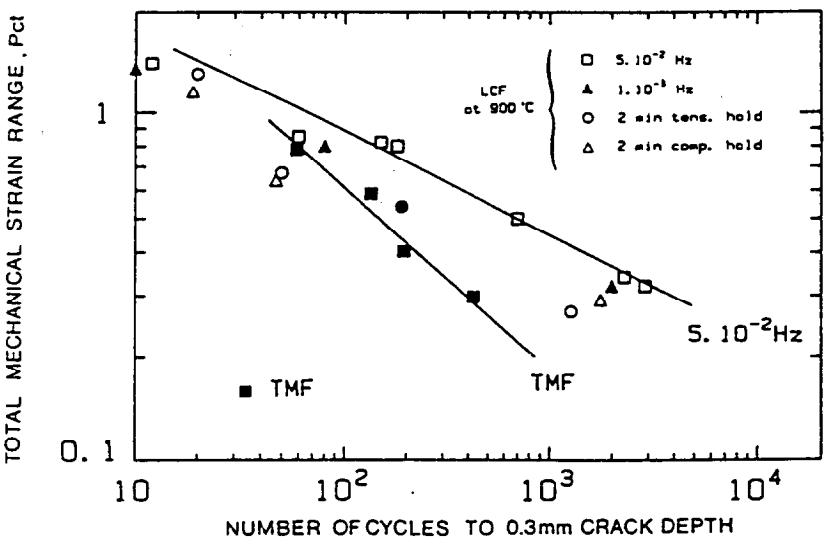

Fig. 5. Comparison of life to 0.3mm crack depth vs total mechanical strain range under TMF cycling and LCF life at 900°C to 0.3mm crack depth under various strain cycles[9].

To summarize, the literature provided a fairly comprehensive indication of the fatigue life of MAR-M509 at the temperatures typically observed in service. Compressive holds, thermal and thermo-mechanical fatigue at similar temperatures and strain ranges were found to be considerably more damaging than low cycle fatigue, and these factors should be taken into account when attempting to predict a component's behaviour in service.

LIFEING ALGORITHMS

When selecting a life evaluation model, its suitablity must be assessed with respect to complexity of application, number and availability of materials constants and suitability of the model to the observed service conditions and failure modes. The performance of several life prediction models, with MAR-M509 as the subject material, is assessed in the literature[7-10]. These models can be broadly classified into the creep models of Robinson and Taira[11] and Franklin[12], strain range partitioning[13], oxidation fatigue[7,8], variations on the Coffin-Manson law, and time and life fraction rules such as that employed in the ASME code N47 [14]. The performance comparison is summarised in ***Table 3***. From this it can be seen that little difference was found between the various models, with only the method of universal slopes being found unsuitable. However, their suitability is not universal, as will be discussed.

Table 3. Performance comparison of life-prediction models[2]

Method	Descriptor	m	s	d_{max}
Universal slopes	$\Delta\varepsilon_{tot}$	0	1.71	615
Ductility Normalized SRP	$\Delta\varepsilon_{in}$	0	0.47	11
Spera	$\varepsilon_{in}(\sigma)$	0	0.24	3.1
Manson-Coffin	$\Delta\varepsilon_{in}$	2	0.39	7.4
Ostergren	$\sigma_{max}\Delta\varepsilon_{in}$	2	0.39	7.4
Manson-Coffin, frequency modified	$\Delta\varepsilon_{in}$	3	0.33	3.8
Ostergren, frequncy modified	$\sigma_{max}\Delta\varepsilon_{in}$	3	0.30	3.3
Analogous to ASME code	$\Delta\varepsilon_{in}\sigma$	4	0.32	4.5
SRP - linear damage rule	$\Delta\varepsilon_{in}$	8	0.33	3.0

m = number of fit parameters; s = standard deviation in log N_f; d_{max} = maximum deviation, defined as maximum value of N_f (calculated)/N_f(measured)

The method of strain range partitioning (SRP), for example, was found to perform about the best with MAR-M509. In the strain range partitioning method, the inelastic strain range is divided into four strain range components: $\Delta\varepsilon_{pp}$ (plastic strain in tension reversed by plastic strain in compression), $\Delta\varepsilon_{pc}$ (plastic strain in tension reversed by creep strain in compression),$\Delta\varepsilon_{cp}$ (creep strain in tension reversed by plastic strain in compression), $\Delta\varepsilon_{cc}$ (creep strain in tension reversed by creep strain in compression). Each type of creep strain is related to creep life according to a Manson-Coffin relation:

$$N_{ij} = A_{ij}\Delta\varepsilon_{ij}^{\alpha_{ij}} \tag{1}$$

Damage is then summed according to a linear damage rule:

$$\frac{1}{N} = \Sigma\frac{1}{N_{ij}} \tag{2}$$

All eight variables for MAR-M509 were supplied in Ref. 7. However, certain practical difficulties immediately become apparent when attempting to use this approach. The method is complicated to use due to the difficulty in separating a cycle into the above components, is difficult to apply when there are small strain amplitudes, and is unable to deal with non-closed loops and non-isothermal cycles[2]. Since superalloy components typically operate under complicated load cycles with frequent thermal transients and little or no plastic strain, this method was deemed to be unsuitable, even though all the required fitting parameters were available.

The creep models were also immediately eliminated since they assume creep damage takes place only in tension. Since the operating stresses in the relevant areas of the component were found to be negligible, and generally compressive, neither of the creep models would have been able to predict a design life in these regions.

Because of the observed failure mode in MAR-M509, The oxidation model proposed by Reuchet and Rémy seemed particularly promising. In this model crack growth is assumed to be the sum of fatigue and oxidation crack growth:

$$\frac{da}{dN} = \left(\frac{da}{dN}\right)_{fat} + \left(\frac{da}{dN}\right)_{ox} \tag{3}$$

The first term was calculated with the expression:

$$\frac{da}{dN} = 0.51\Delta\varepsilon_{in}\left[1/\cos(\pi\sigma/2T) - 1\right] \tag{4}$$

where σ is the peak tensile stress and T is the tensile fracture stress. The oxidation component is calculated by:

$$\frac{da}{dN} = (1-f_c)\alpha_M(1+K_M\Delta\varepsilon_{in})\Delta t^{1/2} + f_c\alpha_c g(\Delta\varepsilon_{in})\Delta t^{1/4} \tag{5}$$

where:

$$g(\Delta\varepsilon_{in}) = 1 \qquad \text{for } \Delta\varepsilon_{in} < \Delta\varepsilon_o$$
$$g(\Delta\varepsilon_{in}) = \Delta\varepsilon_{in}/\Delta\varepsilon_o \qquad \text{for } \Delta\varepsilon_{in} \geq \Delta\varepsilon_o$$

The terms in the above equation refer to the oxidation of the matrix and the carbides respectively. The parameters α_M and α_M are the oxidation constants of the carbides and matrix under zero stress, f_c the volume fraction of carbides in the crack path , K_M and α_C are constants and Δt the cycle period. Once the constants are known, the fatigue life can be calculted by integrating the crack growth equations. However, the meaning of the constants is never described in the paper, making it impossible to apply the above technique. In addition, the use of the Manson-Coffin crack growth criterion of $\Delta\varepsilon_{in}$ renders the use of this model impossible, since no inelastic strains were in fact observed in the component.

As can be seen from Table 3, very good results were obtained from using an approach similar to the ASME N47 code. Furthermore, it is extremely simple to apply. So, for comparative purposes, two commonly applied design rules, the time and life fraction rule used in the ASME code N47[14] and the 10% rule were used. Although not physically based, the simplicity of the codes and their ease of application makes them an attractive option if they can be shown to be suitable for life prediction purposes.

The time and cycle fraction rule - ASME N47

Creep and fatigue are considered to be two distinct processes which can be summed linearly i.e.

$$D = \Sigma\frac{N}{N_f} + \Sigma\frac{t}{t_r} \tag{6}$$

Fatigue damage is calculated by the method of universal slopes:

$$\Delta\varepsilon_{equiv} = \frac{3.5\sigma_u}{E}\left(N_f\right)^{-0.12} + \varepsilon_f\left(N_f\right)^{-0.6} \tag{7}$$

where

$$\Delta\varepsilon_{equiv.} = \frac{\sqrt{2}}{3}\left[\left(\Delta\varepsilon_x - \Delta\varepsilon_y\right)^2 + \left(\Delta\varepsilon_y - \Delta\varepsilon_z\right)^2 + \left(\Delta\varepsilon_z - \Delta\varepsilon_x\right)^2 + \frac{3}{2}\left(\Delta\gamma_{xy}^2 + \Delta\gamma_{yz}^2 + \Delta\gamma_{zx}^2\right)\right]^{1/2} \tag{8}$$

Creep damage is summed throughout the loading cycle using the Larson-Miller equation, and the tensile properties in equation (7) are calculated at the maximum temperature occurring during the cycle.

The 10% rule

The 10% rule was proposed by Manson in order to modify the results of the universal slopes equation (7) to make it suitable for high temperature application. The 10% rule considers only fatigue damage, which is given by:

$$\Delta\varepsilon_t = \frac{3.5\sigma_u}{E}\left(10N_f\right)^{-0.12} + \varepsilon_f\left(10N_f\right)^{-0.6} \tag{9}$$

In this case $\Delta\varepsilon_t$ was taken to be the maximum strain range in the cycle, and the material's tensile properties at the maximum temperature in the cycle were used.

Fatigue Test Data

In addition, the fatigue, TF and TMF data gathered from the literature was used to obtain a rough estimate of cycles to failure. It was imagined that this would produce a rough guide only, since the data had to be extrapolated. As before, the maximum strain range was used, and, in the case of low cycle fatigue, the temperature at which the maximum stress occured was used to extrapolate cycles to failure. The extrapolated LCF data was also compared with the universal slopes relation because fitting this relation to the data in ***Fig. 4*** produced a very good fit of ± 2, and the use of this relation can therefore be justified in pure fatigue applications for this alloy.

In the case of the 10% rule and the fatigue curve fitting, a rainflow algorithm was used to count cycles in load cases where more than one stress/strain cycle was encountered. Cycles to failure were then calculated by:

$$\frac{1}{N_f} = \Sigma\frac{1}{N_{fi}} \tag{10}$$

FINITE ELEMENT MODELS

There are several ways to approach the problem of developing a finite element model of this component. The main focus of interest is of course on the regions experiencing the most severe loading, which occurs on the leading and trailing edges of the vane, at a radial position roughly two-thirds along the vane. Because the sector airfoil was hollow (but not cooled), and the wall of uniform thickness, a 3-dimensional shell model was possible, and this was the preferred route. Another option was to use a 2-dimensional model of the airfoil section. Since the section is uniform throughout, this is a tempting option, and is sometimes seen in the literature. However, while it is reasonable for estimating the metal temperatures at the hottest section, it is far too conservative for predicting the radial stresses when used in plane strain, even when a generalized plane strain option is employed, which allows radial expansion. It was decided nevertheless to use the 2-dimensional approach in parallel with the 3-dimensional, to quantify these errors.

Geometry

Since no drawings or CAD models were available at the commencement of the project, a geometric model of the component was obtained from a Zeiss co-ordinate measuring machine (CMM). The CMM software produced CAD splines which were then passed via an IGES interface to a CAD modeller (Intergraph) where the full component geometry was assembled. A surface model was produced from this, cut down to one vane.

Two meshes were generated initially using an automesh facility:

- a 2-dimensional quadratic mesh representing an airfoil section;
- a single-vaned 3-dimensional linear shell mesh with a finer density in the areas of interest, and 5 integration points at each node.

These meshes were then translated to ABAQUS input decks. The three-dimensional shell mesh is shown in ***Fig. 6***.

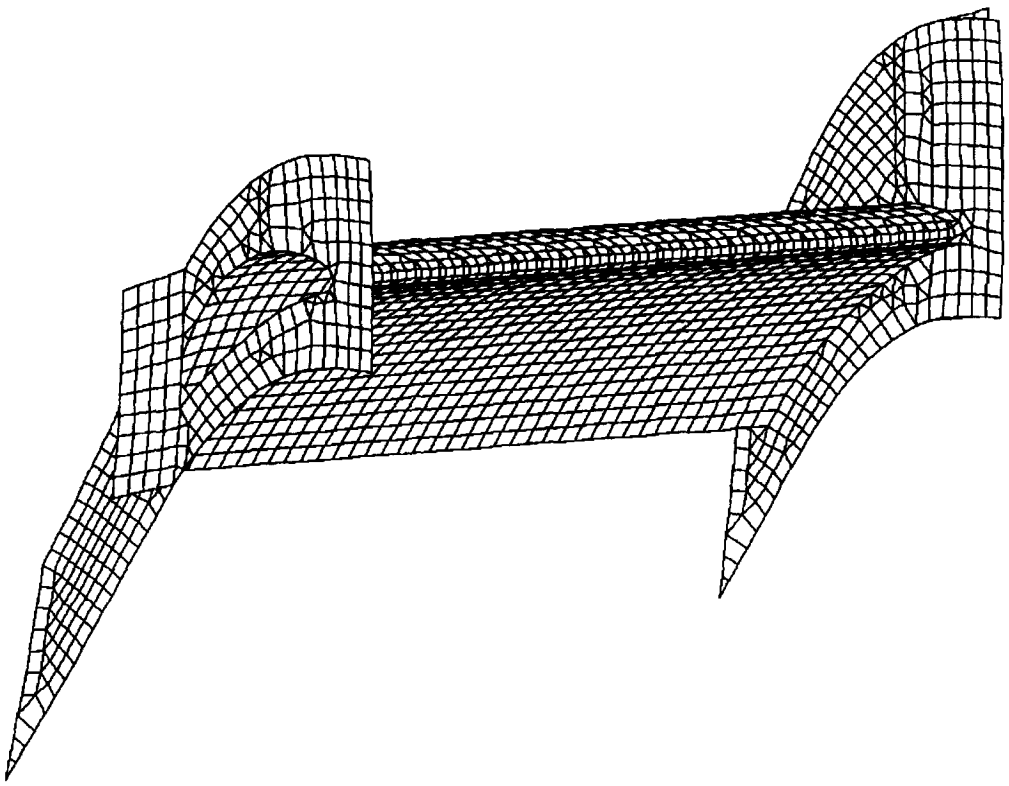

Fig. 6. Mesh used in 3-dimensional Finite Element Analyses

Boundary Conditions

Engine design performance data were available, and these were used as inputs to specialised CFD software codes. The outputs of these codes were gas temperatures and heat transfer coefficients over the vanes. It was decided to apply the approach recommended by the USAF in its ENSIP standard[1], which is to examine two conservative engine operating cycles as a minimum:

- zero - max - zero;
- idle - max / intermediate - idle;

The aim here was to examine likely maximum transient stress and strain ranges for use in the lifeing algorithms, not to simulate an exact mission, since without extensive health monitoring systems in place in the engines in question this would have been very difficult. The CFD analyses were performed assuming 'clean' (new) and 'dirty' (service-exposed) blades. The results presented here used the 'dirty' option, as it was felt that this was both more realistic and more damaging.

The convection boundary conditions necessary for the above analyses were generated and then applied to all relevant element faces using in-house 3-D interpolation software. Transient thermal analyses were performed, and the results passed on to stress analyses. The lifeing algorithms described in the previous section were then applied to the strain history for each of the cycles.

RESULTS

Thermal Analyses

It was immediately apparent from the engine cycle calculations that the 'hot-and-high' operation of these engines was generating very elevated gas temperatures in the turbine. This obviously applied to the idle and maximum (take-off) conditions only. Metal temperatures of up to 970°C were the result. The position of the maxima were seen to be in the correct places relative to the high-damage areas of the retired components.

Static Analyses

The 2-dimensional generalised plane strain model provided reasonably accurate thermal history results, but as expected could not produce the same transient stresses as the 3-dimensional model. ***Figure 7*** presents the thermal results taken from the leading edges of the two models, showing that there is little variation between them. ***Figure 8***, on the other hand, shows quite clearly that the 2-dimensional generalised plane strain model is unable to produce the same strain histories as the three-dimensional mesh.

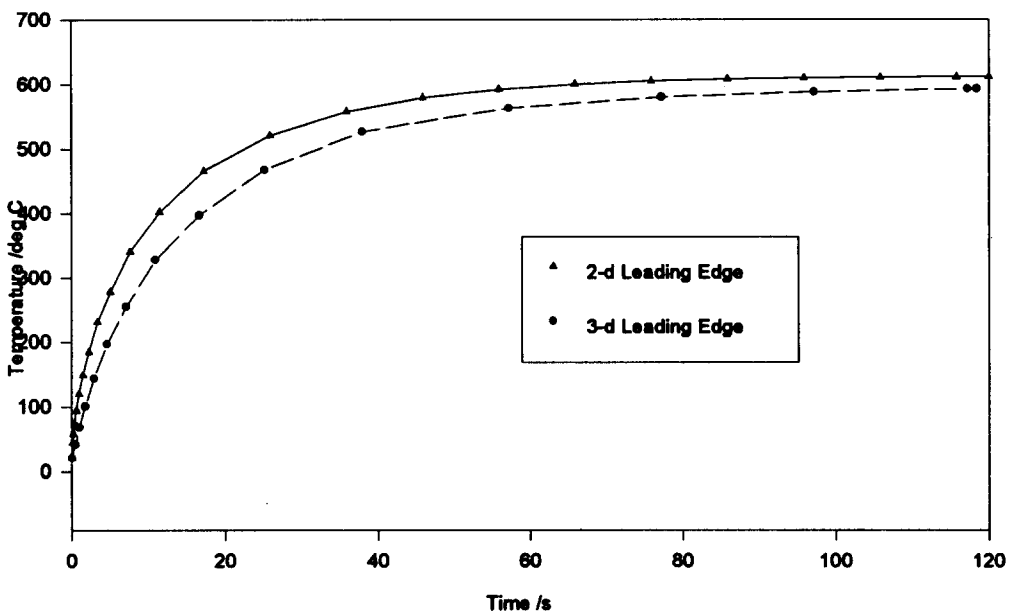

Fig. 7. Thermal histories for 2-d and 3-d FE models (0-idle)

Figure 9 shows the thermal and resultant mechanical strain histories for the 3-d shell model. It is noticeable that the strain amplitudes are low, and under normal operating conditions would cause no significant damage. However, once the alloy has become embrittled due to high temperature exposure, these relatively low strain ranges can cause cracking.

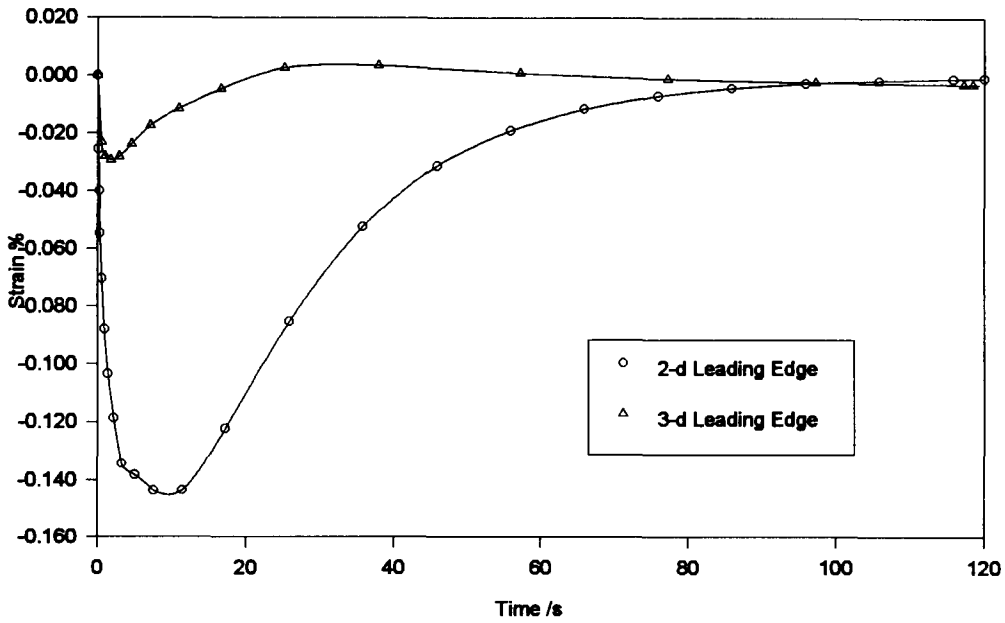

Fig. 8. Comparison of total mechanical strains in the radial direction for the 2-d and 3-d models (0-idle)

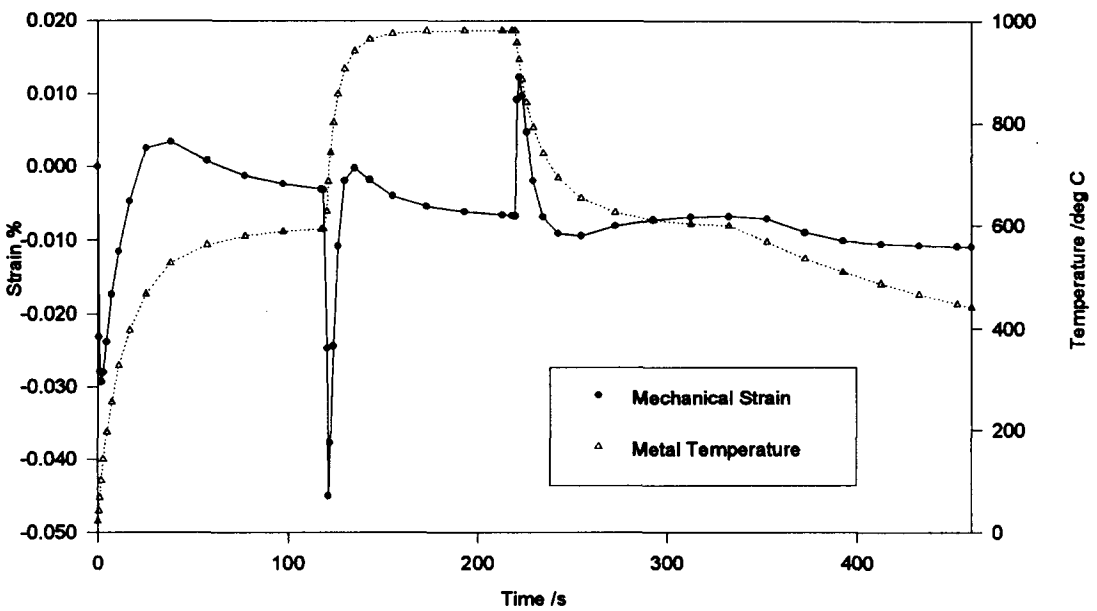

Fig. 9. Strain and temperature histories at leading edge of shell model (0-idle-max-idle)

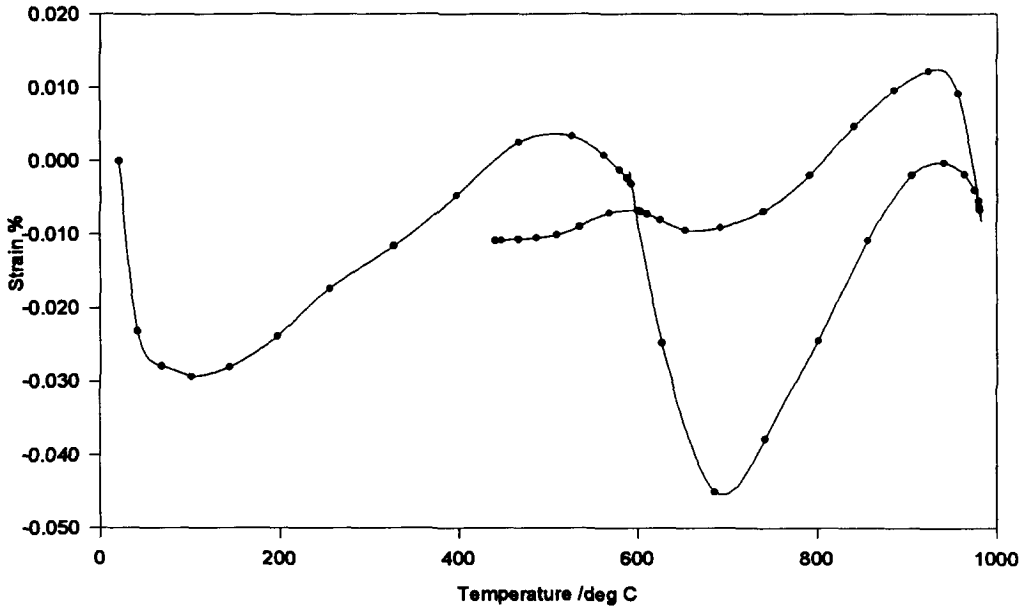

Fig. 10. Strain-temperature relationship at leading edge of shell model (0-idle-max-idle)

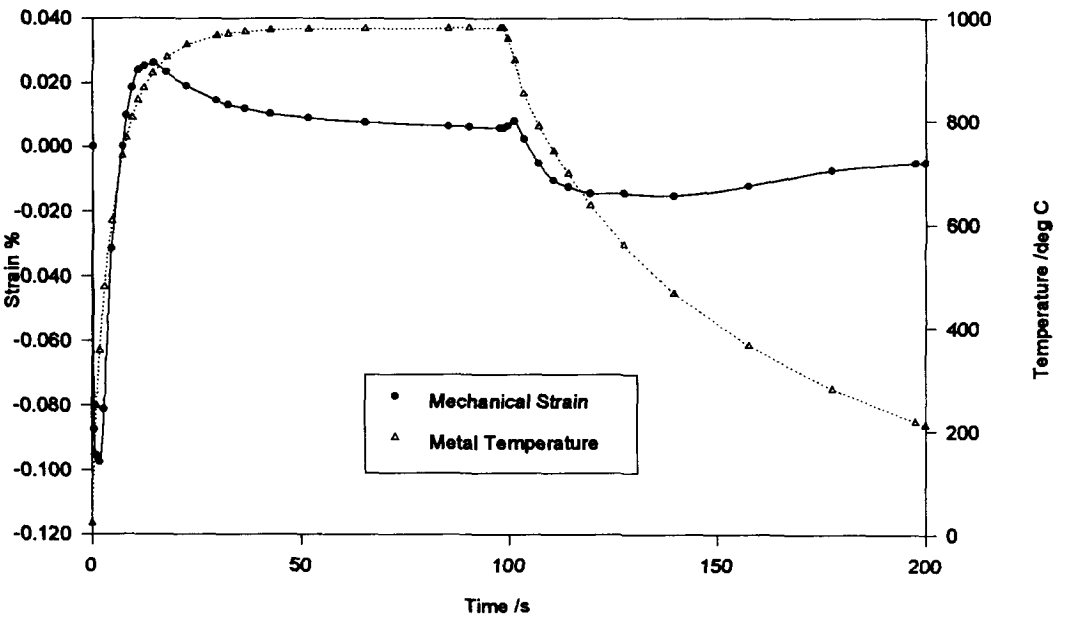

Fig. 11. Strain and temperature histories at leading edge of shell model (0-max-0)

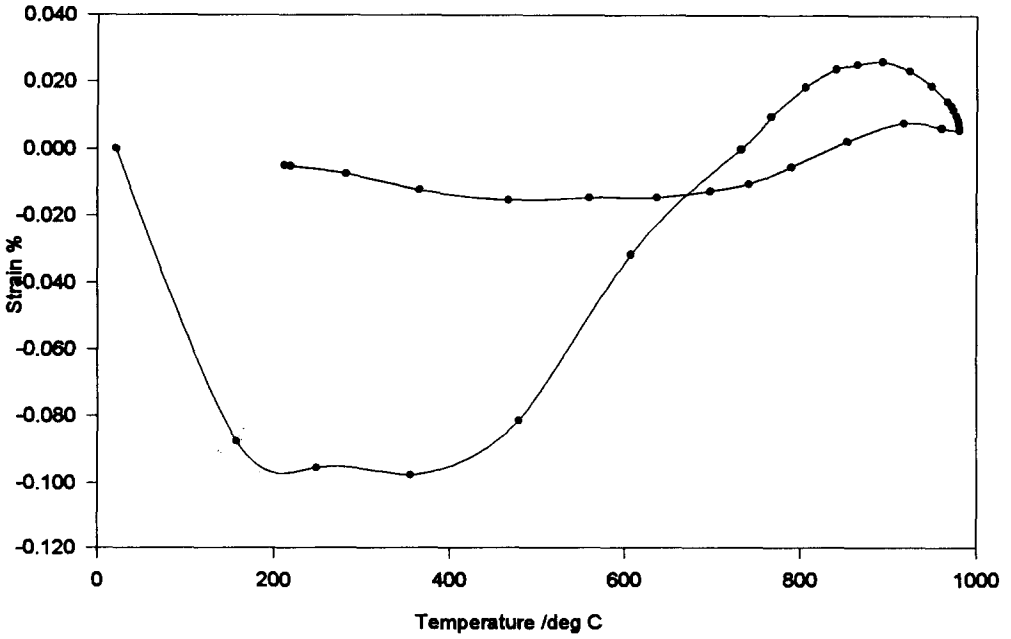

Fig. 12. Strain-temperature relationship at leading edge of shell model (0-max-0)

Results of the lifeing analysis (cycles to failure) are shown in ***Table 4*** below. ASME refers to the ASME code N47 described previously. In this case, no creep damage was observed, and the predicted lifetime is a function of fatigue only. The 10% rule and extrapolated LCF data are also as described previously. In the case of the TF cycle, little extrapolation was required from ***Fig. 4*** in the case of the 0-max-0 cycle, although the difference in temperature accounts for the uncertainty. The TMF cycle required greater extrapolation, although the temperature/strain history is similar to that experienced by the component in the 0-max-0 cycle. No attempt was made to extrapolate the 0-idle-max-idle cycle results, since the strain amplitude is considerably lower than the test conditions.

Table 4. Summary of Lifeing Analysis Results

Cycle	ASME Case N47	10%	LCF	Universal Slopes	TF	TMF*
0-max-0	3.5e7	9.2e5	1.6e5	2.2e6	2000-4000	≈1800
0-idle-max-0	>1.0e8	1.48e7	1.61e6	>1.0e8	not computed	not computed

*Cycles to crack extension of 0.3mm. All others to 1mm

What is clear from the above results is that conventional methods of establishing design life are inadequate for describing time at temperature effects other than creep. The results

from the TF and TMF extrapolations are a great deal more promising, although it must be borne in mind that the simulated 0-max-0 cycle is a great deal more severe than anything experienced in service. Clearly what is required is a model that accounts for the precipitation and oxidation of carbides in combination with materials testing using realistic strain/temperature cycles.

CONCLUSIONS

It was suspected at the beginning of this analysis that the components had been exposed to very high temperatures during operation. Although it was known that the sustained 'hot-and-high' operating conditions of these engines were damaging, it was clear once accurate CFD analyses had been performed that vane metal temperatures were in excess of the expected values, reaching local peaks of 970°C. Under these conditions the vane alloy MAR-M509 is subjected to degradation of its fatigue resistance due to the build-up of MC carbides on its grain boundaries. However, it is also clear that standard lifeing algorithms would not have predicted the resultant reduction in life without materials data which could account for this mechanism at such elevated temperatures.

ACKNOWLEDGEMENTS

The CFD analyses were performed by Mr Thomas Roos of Aerotek, CSIR. Mr Jeff Benson of Mattek, CSIR conducted the metallurgical investigations, while Mr Jaco de la Rouviere, also of Mattek, facilitated the CMM-to-CAD link for the component geometry. Mr Rory Mapstone of Instrumach provided valuable engine operating data, as did Lt-Col Steve Glass of the South African Air Force. The 3-D interpolation software was written by Mr Paul Kotschy of Mattek.

REFERENCES

1. USAF MIL-STD 1783 Engine Structural Integrity Program (1984)
2. Fischmeister, H.F., Danzer, R. and Buchmayer, B. Life Time Prediction Models. *High Temperature Alloys for Gas Turbine and Other Applications,* 1986, 459-549.
3. Wheaton, H.L. MAR-M509, a New Cast Cobalt-based Alloy for High Temperature Service. *Cobalt*, **29**, December 1965, 163-170.
4. ASTM. *Metals Handbook*, vol. 3, 264-265.
5. Viswanathan, R. *Damage Mechanisms and Life Assessment of High Temperature Components,* ASM International, 1989, 415-479.
6. Beck, C.G. and Santhanam, A.T. Effect of Microstructure on the Thermal Fatigue Resistanc of a Cast Cobalt-Base Alloy, MAR-M509. *Thermal Fatigue of Materials and Components,* ASTM STP 612, D.A. Spera and D.F. Mowbray, Eds. American Society for Testing and Materials, 1976, 123-140.
7. Remy, L., Rezai-Aria, F., Danzer, R and Hoffelner, W. Comparison of Life Prediction Methods in MAR-M509 Under High Temperature Fatigue. *High Temperature Alloys for Gas Turbine and Other Applications*, 1986, 1617-1628.

8. Rezai-Aria, F., Dambrine, B. and Remy, L. Thermal Fatigue of MAR-M509 Superalloy - II. Evaluation of Life Prediction Models. *Fatigue Fract. Engng Mater. Struct.* Vol. 11, No. 4, 1988, 291-302.
9. François, M. and Rémy, L. Thermal-Mechanical Fatigue of MAR-M509 Superalloy. Comparison with Low Cycle Fatigue Behaviour. *Fatigue Fract. Engng Mater. Struct.* Vol. 11, No. 4, 1991, 115-129.
10. Rémy, L; Reger, M; Reuchet, J and Rezai-Aria, F. An Operational Definition of Life to Crack Initiation in High Temperature Fatigue. *High Temperature Alloys for Gas Turbine Applications,* R Brunetaud, D Coutsouradis, TB Gibbons, Y Lindblom, DB Meadowcroft and R Stickler, Eds,1982, 619-632.
11. Spera, D.A. *Fatigue at Elevated Temperature.* ASTM STP 520, American Society for Testing and Materials, 1973, 648-657.
12. Franklin, C.J. Cyclic Creep and Fatigue Life Time Prediction. *High Temperature Alloys for Gas Turbines.* D Coutsosradis, P Felix, H Fischmeister, L Habrakin, Y lindblom and M.O. Speidel, Eds, 1978, 513-547.
13. Manson, S.S. *Fatigue at Elevated Temperatures*, ASTM STP 520, American Society for Testing and Materials, 1973, 744-782.
14. ASME N47-19. Cases of ASME Boiler and Pressure Vessel Code.